Applied Mathematics and Computation 377 (2020) 125158

Contents lists available at ScienceDirect

Applied Mathematics and Computation

journal homepage: www.elsevier.com/locate/amc

Spatial dynamics of an epidemic model with nonlocal infection

Zun-Guang Guo[a,b,c], Gui-Quan Sun[b,d,*], Zhen Wang[e,*], Zhen Jin[d], Li Li[f], Can Li[c]

[a] Data Science and Technology, North University of China, Shanxi, Taiyuan 030051, PR China
[b] Department of Mathematics, North University of China, Shanxi, Taiyuan 030051, PR China
[c] Department of Science, Taiyuan Institute of Technology, Shanxi, Taiyuan 030008, PR China
[d] Complex Systems Research Center, Shanxi University, Shanxi, Taiyuan 030006, PR China
[e] School of Mechanical Engineering and Center for OPTical IMagery Analysis and Learning (OPTIMAL), Northwestern Polytechnical University, Xi'an 710072, PR China
[f] School of Computer and Information Technology, Shanxi University Taiyuan, Shanxi 030006, PR China

ARTICLE INFO

Article history:
Received 14 December 2019
Revised 6 February 2020
Accepted 9 February 2020

Keywords:
Nonlocal delay
Disease transmission
Turing pattern
Multi-scale analysis

ABSTRACT

Nonlocal infection plays an important role in epidemic spread, which can reflect the real rules of infectious disease. To understand its mechanism on disease transmission, we construct an epidemic model with nonlocal delay and logistic growth. The Turing space for the emergence of stationary pattern is determined by series of inequations by mathematical analysis. Moreover, we use the multi-scale analysis to derive the amplitude equation, and obtain rich pattern structures by controlling the variation of the delay parameter. As the increase of delay parameter, the degree of pattern isolation increase as well as the density of the infected population decrease which prohibits the propagation of the disease in space. The results systematically reveal the impact of nonlocal delay on the spread of infectious diseases and provide some new theoretical supports for controlling the spread of infectious diseases.

1. Introduction

The spread of infectious diseases is harmful to human health and hinders social and economic development [1,2]. Therefore, it is necessary to study the transmission law of infectious diseases [3–6]. The incidence rate plays a vital role in modelling infectious diseases since it approximately reflects the interactions between susceptible and infectious individuals. The incidence rate $g(I)S$ can take into account many factors of affecting diseases spread, such as individual activity ability, environmental conditions and the virulence of the virus, which depends on the real diseases and environments. Most of researchers used the simply bilinear incidence rate $g(I)S = \beta SI$ based on the mass action law [7–14]. However, when the volume of infectious individuals reaches a high level, infectivity generally tends to a constant. So some work adopted the saturation incidence $g(I)S = \frac{\beta IS}{1+kI}$ [15–20]. Liu et al. [21] proposed a more general nonlinear incidence rate $g(I)S = \frac{\beta I^p S}{1+kI^q}$, where βI^p represents the infectivity of infectious diseases, and $\frac{1}{1+kI^q}$ reflects the behavior change when susceptible individuals increase or the suppression result of crowding effect of infectious individuals. This nonlinear incidence rate was

* Corresponding authors.
E-mail addresses: gquansun@126.com (G.-Q. Sun), w-zhen@nwpu.edu.cn (Z. Wang).

https://doi.org/10.1016/j.amc.2020.125158
0096-3003/

then applied by many researchers [22–26]. Ruan and Wang [27] took the incidence rate $g(I)S = \frac{\beta I^2 S}{1+kI^2}$ to study the global dynamics of one class of SIR models. Some researchers also introduced other nonlinear incidence rates (referred to [28–35]).

All research of infectious diseases spread mentioned above is based on local contagion, that is to say, the susceptible are infected by the infectious at the current time and position. The introduction of nonlocal delay challenges many existing research methods on reaction-diffusion equations. At the same time, many essential changes in dynamic behavior caused by nonlocal delay are also found in the research process. Nonlocal reaction-diffusion equation is considered to be a more accurate description of natural phenomena in physics, ecology and infectious diseases. During the spread of the disease, many diseases may be transmitted by air flow, vectors or migration. It means that the newly infectious individuals per time depend not only on the number of the infectious at the current time and position, but also on the number of infectious individuals at total space. This infection action is called nonlocal interaction, denoted by

$$g(I) = \beta \int_{\Omega} \int_{-\infty}^{t} Q(x-y, t-s) I(y,s) ds dy,$$

where Ω represents the total space and $Q(x-y, t-s)$ represents the influence size of infectious individuals at s time and y position to susceptible individuals at t time and x position. It takes s unit times from position y to position x. Theoretically, the model established after considering these factors will be more realistic. From the point of view of modelling, the introduction of nonlocal delay is a very effective and important approach to model disease transmission. As a result, we will establish the model based on this incidence rate.

Partial differential equation (PDE) is generally used to establish epidemic model with the heterogeneous distribution of susceptible and infectious individuals at space. Pattern of infectious diseases is the heterogeneous macroscopic structure with some laws that epidemic contagion shows at time or space. These approaches can be used by reaction-diffusion equations to study the dynamics of infectious diseases [36–42]. The pattern is the crucial index of epidemic spreading at space, from which, the density distribution of infectious individuals at space can be seen. So one can find the hot area of infectious diseases, and can also see whether the space structure of infectious diseases is stable. The pattern structure will further provide important guidelines for prevention and control of infectious diseases.

Currently, most work studied the global solution, traveling wave solution or wave train solution of models with nonlocal (or nonlocal delay) interaction [43–62]. Few focus on pattern dynamics of reaction-diffusion equations with nonlocal delays term. In particular, we have proposed a class of SIS models with nonlocal delays [63]:

$$\begin{cases} \dfrac{\partial S}{\partial t} = D_S \Delta S + B - \beta S\left(\int_{R^2} \int_{-\infty}^{t} Q(x-y, t-s) I(y,s) ds dy\right)^2 - \mu S + \gamma I, \\ \dfrac{\partial I}{\partial t} = D_I \Delta I + \beta S\left(\int_{R^2} \int_{-\infty}^{t} Q(x-y, t-s) I(y,s) ds dy\right)^2 - \gamma I - dI - \mu I. \end{cases} \tag{1.1}$$

We studied some pattern dynamics of model. However, we did not find out what pattern structure will appear in some specific parameter regions. Also, it is actually more realistic by using logistic birth [67–69]. Therefore, in this paper, we proposed the following model:

$$\begin{cases} \dfrac{\partial S}{\partial t} = D_S \Delta S + r(S+I)\left(1 - \dfrac{S+I}{K}\right) - \beta S \dfrac{\int_{R^2} \int_{-\infty}^{t} Q(x-y, t-s) I(y,s) dy ds}{S+I} - (\mu + A) S, \\ \dfrac{\partial I}{\partial t} = D_I \Delta I + \beta S \dfrac{\int_{R^2} \int_{-\infty}^{t} Q(x-y, t-s) I(y,s) dy ds}{S+I} - (\mu + d) I, \end{cases} \tag{1.2}$$

where $S(x, t)$ and $I(x, t)$ denote the densities of the susceptible and the infected at position $x (x \in R^2)$ and at time t, respectively. D_S, D_I are diffusion rate, $\Delta = \frac{\partial^2}{\partial X^2} + \frac{\partial^2}{\partial Y^2}$, β is infection rate, μ is natural mortality, d is due to disease mortality, r is the intrinsic growth rate, K is the carrying capacity, A is the migration rate of susceptible population. This paper is based on the random movement of individuals, and the kernel function is taken as:

$$Q(x,t) = \frac{1}{4\pi t} \exp\left(-\frac{|x|^2}{4t}\right) \frac{1}{\tau} \exp\left(-\frac{t}{\tau}\right).$$

The paper is organized as follows. In the second section, we performed linearization analysis and bifurcation analysis for the model, and obtained the conditions of the Turing Bifurcation. In the third section, we perform multi-scale analysis near the critical value τ_T of the control parameter τ, and derive the amplitude equation that can reflect the structure of the pattern. In the fourth section, we performed numerical simulations and obtained a rich Turing pattern and explained it. In the last part, we summarize the results of the simulation.

2. Mathematical analysis

In this part, we will show detailed analysis on system (1.2). Let $V(x,t)=\int_{R^2}\int_{-\infty}^{t}Q(x-y,t-s)I(y,s)dyds$, system (1.2) will become the following form:

$$\begin{cases}\dfrac{\partial S}{\partial t}=D_S\Delta S+r(S+I)\left(1-\dfrac{S+I}{K}\right)-\dfrac{\beta SV}{S+I}-(\mu+A)S,\\ \dfrac{\partial I}{\partial t}=D_I\Delta I+\dfrac{\beta SV}{S+I}-(\mu+d)I,\\ \dfrac{\partial V}{\partial t}=\Delta V+\dfrac{1}{\tau}(I-V).\end{cases}\tag{2.1}$$

By dimensional change, the equations are obtained:

$$\begin{cases}\dfrac{\partial S}{\partial t}=d_1\Delta S+R_d\nu_{SI}(S+I)(1-(S+I))-R_0\dfrac{SV}{S+I}-\nu_{SI}S,\\ \dfrac{\partial I}{\partial t}=d_2\Delta I+R_0\dfrac{SV}{S+I}-I,\\ \dfrac{\partial V}{\partial t}=d_3\Delta V+\frac{1}{\tau}(I-V),\end{cases}\tag{2.2}$$

where

$$R_0=\frac{\beta}{\mu+d},R_d=\frac{r}{\mu+A},\nu_{SI}=\frac{\mu+A}{\mu+d}.$$

System (2.2) has a disease free equilibrium $E_0=(S_0,I_0,V_0)=(\frac{R_d-1}{R_d},0,0)$. At the same time, there is an endemic equilibrium $E^*=(S^*,I^*,V^*)$ with

$$S^*=\frac{R_dR_0\nu_{SI}-R_0-\nu_{SI}+1}{R_dR_0^2\nu_{SI}},$$

$$I^*=\frac{R_dR_0^2\nu_{SI}-R_dR_0\nu_{SI}-R_0^2-R_0\nu_{SI}+2R_0+\nu_{SI}-1}{R_dR_0^2\nu_{SI}},$$

$$V^*=I^*.$$

Here, we mainly concern about the dynamical behavior near the endemic equilibrium point. Therefore, the following study only focuses on the endemic equilibrium point E^*.

One linearized system (2.2) at the coexistence steady state E^* and obtained the following system:

$$\begin{cases}\dfrac{\partial S}{\partial t}=d_1\Delta S+a_{11}S+a_{12}I+a_{13}V,\\ \dfrac{\partial I}{\partial t}=d_2\Delta I+a_{21}S+a_{22}I+a_{23}V,\\ \dfrac{\partial V}{\partial t}=d_3\Delta V+a_{31}S+a_{32}I+a_{33}V,\end{cases}\tag{2.3}$$

where

$$a_{11}=-\frac{R_dR_0\nu_{SI}+R_0^2+R_0\nu_{SI}-4R_0-2\nu_{SI}+3}{R_0},$$

$$a_{12}=-\frac{R_dR_0\nu_{SI}-3R_0-2\nu_{SI}+3}{R_0},a_{13}=-1,$$

$$a_{21}=\frac{(R_0-1)^2}{R_0},a_{22}=\frac{1-2R_0}{R_0},a_{23}=1,$$

$$a_{31}=0,a_{32}=\frac{1}{\tau},a_{33}=-\frac{1}{\tau}.$$

Let

$$\begin{pmatrix} S \\ I \\ V \end{pmatrix} = \begin{pmatrix} C_k^1 \\ C_k^2 \\ C_k^3 \end{pmatrix} \exp(\lambda t + i\vec{k}\cdot\vec{r}), \tag{2.4}$$

where $\vec{r} = (X, Y)$, $\vec{k} = (k_X, k_Y)$, and the number of wave is $k = \sqrt{k_X^2 + k_Y^2}$. λ is the growth rate of perturbation in time t. Combining (2.3) with (2.4), the characteristic equation is given:

$$detA = \begin{vmatrix} a_{11} - d_1k^2 - \lambda & a_{12} & a_{13} \\ a_{21} & a_{22} - d_2k^2 - \lambda & a_{23} \\ a_{31} & a_{32} & a_{33} - d_3k^2 - \lambda \end{vmatrix} = 0,$$

which is equivalent as follows:

$$\lambda^3 + b_1(k)\lambda^2 + b_2(k)\lambda + b_3(k) = 0, \tag{2.5}$$

with

$$\begin{aligned}
b_1(k) =& \frac{1}{R_0\tau}(R_0d_1k^2\tau + R_0d_2k^2\tau + R_dR_0\tau\nu_{SI} + R_0d_3k^2\tau + R_0^2\tau + R_0\tau\nu_{SI} - 2R_0\tau - 2\tau\nu_{SI} + R_0 + 2\tau),\\
b_2(k) =& \frac{1}{R_0\tau}(R_0d_1d_2k^4\tau + R_0d_1d_3k^4\tau + R_0d_2d_3k^4\tau + R_dR_0d_2k^2\tau\nu_{SI} + R_dR_0d_3k^2\tau\nu_{SI} + R_0^2d_2k^2\tau + R_0^2d_3k^2\tau\\
&+ R_0d_2k^2\tau\nu_{SI} + R_0d_3k^2\tau\nu_{SI} + R_dR_0^2\tau\nu_{SI} + 2R_0d_1k^2\tau - 4R_0d_2k^2\tau - 2R_0d_3k^2\tau - 2d_2k^2\tau\nu_{SI} - 2d_3k^2\tau\nu_{SI}\\
&+ R_0d_1k^2 + R_0d_2k^2 - d_1k^2\tau + 3d_2k^2\tau + 2d_3k^2\tau + R_dR_0\nu_{SI} - R_0^2\tau + R_0^2 + R_0\nu_{SI} - \tau\nu_{SI} - 3R_0 + \tau - 2\nu_{SI} + 2),\\
b_3(k) =& \frac{1}{R_0\tau}(R_0d_1d_2d_3k^6\tau + R_dR_0d_2d_3k^4\tau\nu_{SI} + R_0^2d_2d_3k^4\tau + R_0d_2d_3k^4\tau\nu_{SI} + R_dR_0^2d_3k^2\tau\nu_{SI} + 2R_0d_1d_3k^4\tau\\
&- 4R_0d_2d_3k^4\tau - 2d_2d_3k^4\tau\nu_{SI} + R_0d_1d_2k^4 - d_1d_3k^4\tau + 3d_2d_3k^4\tau + R_dR_0d_2k^2\nu_{SI} - R_0^2d_3k^2\tau + R_0^2d_2k^2\\
&+ R_0d_2k^2\nu_{SI} - d_3k^2\tau\nu_{SI} + R_dR_0^2\nu_{SI} + R_0d_1k^2 - 4R_0d_2k^2 - 2d_2k^2\nu_{SI} + d_3k^2\tau - R_dR_0\nu_{SI} - d_1k^2 + 3d_2k^2 - R_0^2\\
&- R_0\nu_{SI} + 2R_0 + \nu_{SI} - 1).
\end{aligned}$$

If system (2.3) has no diffusion term, the corresponding characteristic equation is as follows:

$$\sigma^3 + b_1(0)\sigma^2 + b_2(0)\sigma + b_3(0) = 0, \tag{2.6}$$

where

$$\begin{aligned}
b_1(0) =& \frac{1}{R_0\tau}(R_dR_0\tau\nu_{SI} + R_0^2\tau + R_0\tau\nu_{SI} - 2R_0\tau - 2\tau\nu_{SI} + R_0 + 2\tau),\\
b_2(0) =& \frac{1}{R_0\tau}(R_dR_0^2\tau\nu_{SI} + R_dR_0\nu_{SI} - R_0^2\tau + R_0^2 + R_0\nu_{SI} - \tau\nu_{SI} - 3R_0 + \tau - 2\nu_{SI} + 2),\\
b_3(0) =& \frac{1}{R_0\tau}(R_dR_0^2\nu_{SI} - R_dR_0\nu_{SI} - R_0^2 - R_0\nu_{SI} + 2R_0 + \nu_{SI} - 1).
\end{aligned}$$

By the Huriwitz criterion, the condition of stability of E^* in system(2.3) without diffusion is given as follows:

$$\begin{cases} b_1(0) > 0, \\ b_3(0) > 0, \\ b_1(0)b_2(0) - b_3(0) > 0. \end{cases} \tag{2.7}$$

The necessary conditions for the Turing pattern to appear near the equilibrium point E^* are: The equilibrium E^* of system (2.2) is locally stable without diffusion; While E^* becomes unstable in system (2.3).

Next, we analyze the conditions with system (2.3) occurring Turing patterns from three cases.

Case 1. $b_1(k) > 0$

$$b_1(k) = \frac{1}{R_0\tau}(R_0d_1k^2\tau + R_0d_2k^2\tau + R_dR_0\tau\nu_{SI} + R_0d_3k^2\tau) + b_1(0).$$

Since all the coefficients in model (2.2) are non-negative, the case 1 is always established under the condition $b_1(0) > 0$.

Case 2. $b_3(k) > 0$.

Let $b_3(k) = H_2(k^2)$ and $z = k^2$, then $H_2(z) = h_3z^3 + h_2z^2 + h_1z + h_0$, where

$$h_3 = d_1d_2d_3,$$

$$h_2 = \frac{1}{R_0\tau}(R_dR_0d_2d_3\tau\nu_{SI} + R_0^2d_2d_3\tau + R_0d_2d_3\tau\nu_{SI} + 2R_0d_1d_3\tau - 4R_0d_2d_3\tau - 2d_2d_3\tau\nu_{SI} + R_0d_1d_2 - d_1d_3\tau + 3d_2d_3\tau),$$

$$h_1 = \frac{1}{R_0\tau}(R_dR_0^2d_3\tau\nu_{SI} + R_dR_0d_2\nu_{SI} - R_0^2d_3\tau + R_0^2d_2 + R_0d_2\nu_{SI} - d_3\tau\nu_{SI} + R_0d_1 - 4R_0d_2 - 2d_2\nu_{SI} + d_3\tau - d_1 + 3d_2),$$

$$h_0 = \frac{1}{R_0\tau}(R_0 - 1)(R_dR_0\nu_{SI} - R_0 - \nu_{SI} + 1).$$

Two properties of $H_2(z)$ are easy to know from the basic properties of polynomials:

Property 1. *When z tends to be positive infinity, the function value of $H_2(z)$ tends to be positive infinity.*

Property 2. *$H_2(z)$ has two extreme points, denoted as $z_{21} = \frac{-h_2+\sqrt{(h_2)^2-3h_3h_1}}{3h_3}$ and $z_{22} = \frac{-h_2-\sqrt{(h_2)^2-3h_3h_1}}{3h_3}$. $H_2(z)$ takes a minimum value at point z_{21} and a maximum at point z_{22}, and their size relationship is*

$$z_{2,\max} = z_{22} < z_{2,\min} = z_{21}.$$

If the Turing bifurcation occurs, the condition $H_2(z_{2,\min}) = H_2(z_{21}) < 0$ should be satisfied. Since that $z_{2,\min} = z_{21} = \frac{-h_2+\sqrt{(h_2)^2-3h_3h_1}}{3h_3}$ represents a physical wave number, and $z_{2,\min} = z_{21}$ is positive. The value of expression under the quadratic square root must be positive, i.e., $(h_2)^2 - 3h_3h_1 > 0$. In conclusion, the conditions that induce the Turing bifurcation are as follows:

$$\begin{cases} (h_2)^2 - 3h_3h_1 > 0, \\ z_{2,\min} = z_{21} > 0, \\ H_2(z_{2,\min}) = H_2(z_{21}) < 0, \\ H_2(0) = b_3(0) > 0, \\ b_1(0)b_2(0) - b_3(0) > 0, \\ b_1(0) > 0. \end{cases} \tag{2.8}$$

Case 3. $b_1(k)b_2(k) - b_3(k) > 0$. Let $b_1(k)b_2(k) - b_3(k) = H_3(k^2)$ and $z = k^2$, then $H_3(z) = h_{q_3}z^3 + h_{q_2}z^2 + h_{q_1}z + h_{q_0}$, with

$$h_{q_3} = (d_2 + d_3)(d_1 + d_3)(d_1 + d_2),$$

$$\begin{aligned} h_{q_2} =& \frac{1}{R_0\tau}(2R_dR_0d_1d_2\tau\nu_{SI} + 2R_dR_0d_1d_3\tau\nu_{SI} + R_dR_0d_2^2\tau\nu_{SI} + 2R_dR_0d_2d_3\tau\nu_{SI} + R_dR_0d_3^2\tau\nu_{SI} + 2R_0^2d_1d_2\tau + 2R_0^2d_1d_3\tau \\ &+ R_0^2d_2^2\tau + 2R_0^2d_2d_3\tau + R_0^2d_3^2\tau + 2R_0d_1d_2\tau\nu_{SI} + 2R_0d_1d_3\tau\nu_{SI} + R_0d_2^2\tau\nu_{SI} + 2R_0d_2d_3\tau\nu_{SI} + R_0d_3^2\tau\nu_{SI} + 2R_0d_1^2\tau \\ &- 4R_0d_1d_2\tau - 4R_0d_1d_3\tau - 4R_0d_2^2\tau - 4R_0d_2d_3\tau - 2R_0d_3^2\tau - 4d_1d_2\tau\nu_{SI} - 4d_1d_3\tau\nu_{SI} - 2d_2^2\tau\nu_{SI} - 4d_2d_3\tau\nu_{SI} \\ &- 2d_3^2\tau\nu_{SI} + R_0d_1^2 + 2R_0d_1d_2 + 2R_0d_1d_3 + R_0d_2^2 + 2R_0d_2d_3 - d_1^2\tau + 4d_1d_2\tau + 4d_1d_3\tau + 3d_2^2\tau + 4d_2d_3\tau + 2d_3^2\tau), \end{aligned}$$

$$\begin{aligned} h_{q_1} =& \frac{1}{R_0^2\tau^2}(R_d^2R_0^2d_2\tau^2\nu_{SI}^2 + R_d^2R_0^2d_3\tau^2\nu_{SI}^2 + R_dR_0^3d_1\tau^2\nu_{SI} + 3R_dR_0^3d_2\tau^2\nu_{SI} + 2R_dR_0^3d_3\tau^2\nu_{SI} + 2R_d^2R_0^2d_2\tau^2\nu_{SI}^2 + 2R_d^2R_0^2d_3\tau^2\nu_{SI}^2 \\ &+ 2R_dR_0^2d_1\tau^2\nu_{SI} - 6R_dR_0^2d_2\tau^2\nu_{SI} - 4R_dR_0^2d_3\tau^2\nu_{SI} - 4R_dR_0d_2\tau^2\nu_{SI}^2 - 4R_dR_0d_3\tau^2\nu_{SI}^2 + R_0^4d_2\tau^2 + R_0^4d_3\tau^2 \\ &+ 2R_0^3d_2\tau^2\nu_{SI} + 2R_0^3d_3\tau^2\nu_{SI} + R_0^2d_2\tau^2\nu_{SI}^2 + R_0^2d_3\tau^2\nu_{SI}^2 + 2R_dR_0^2d_1\tau\nu_{SI} + 2R_dR_0^2d_2\tau\nu_{SI} + 2R_dR_0^2d_3\tau\nu_{SI} \\ &- R_dR_0d_1\tau^2\nu_{SI} + 5R_dR_0d_2\tau^2\nu_{SI} + 4R_dR_0d_3\tau^2\nu_{SI} + R_0^3d_1\tau^2 - 7R_0^3d_2\tau^2 - 4R_0^3d_3\tau^2 + 2R_0^2d_1\tau^2\nu_{SI} - 10R_0^2d_2\tau^2\nu_{SI} \\ &- 8R_0^2d_3\tau^2\nu_{SI} - 4R_0d_2\tau^2\nu_{SI}^2 - 4R_0d_3\tau^2\nu_{SI}^2 + 2R_0^3d_1\tau + 2R_0^3d_2\tau + 2R_0^3d_3\tau - 5R_0^2d_1\tau^2 + 2R_0^2d_1\tau\nu_{SI} + 13R_0^2d_2\tau^2 \\ &+ 2R_0^2d_2\tau\nu_{SI} + 8R_0^2d_3\tau^2 + 2R_0^2d_3\tau\nu_{SI} - 6R_0d_1\tau^2\nu_{SI} + 16R_0d_2\tau^2\nu_{SI} + 12R_0d_3\tau^2\nu_{SI} + 4d_2\tau^2\nu_{SI}^2 + 4d_3\tau^2\nu_{SI}^2 \\ &- 4R_0^2d_1\tau - 5R_0^2d_2\tau - 5R_0^2d_3\tau + 7R_0d_1\tau^2 - 4R_0d_1\tau\nu_{SI} - 13R_0d_2\tau^2 - 4R_0d_2\tau\nu_{SI} - 8R_0d_3\tau^2 - 4R_0d_3\tau\nu_{SI} \\ &+ 2d_1\tau^2\nu_{SI} - 10d_2\tau^2\nu_{SI} - 8d_3\tau^2\nu_{SI} + R_0^2d_1 + R_0^2d_2 + 4R_0d_1\tau + 4R_0d_2\tau + 4R_0d_3\tau - 2d_1\tau^2 + 6d_2\tau^2 + 4d_3\tau^2), \end{aligned}$$

$$\begin{aligned} h_{q_0} =& \frac{1}{R_0^2\tau^2}(R^2R_0^3\tau^2\nu_{SI}^2 + R_dR_0^4\tau^2\nu_{SI} + R_dR_0^3\tau^2\nu_{SI}^2 + R_d^2R_0^2\tau\nu_{SI}^2 - 3R_dR_0^3\tau^2\nu_{SI} - 2R_d^2R_0^2\tau^2\nu_{SI}^2 + 2R_dR_0^3\tau\nu_{SI} + 2R_dR_0^2\tau^2\nu_{SI} \\ &+ 2R_dR_0^2\tau\nu_{SI}^2 - R_dR_0\tau^2\nu_{SI}^2 - R_0^4\tau^2 - R_0^3\tau^2\nu_{SI} - 4R_dR_0^2\tau\nu_{SI} + R_dR_0\tau^2\nu_{SI} - 4R_dR_0\tau\nu_{SI}^2 + R_0^4\tau + 2R_0^3\tau^2 + 2R_0^3\tau\nu_{SI} \\ &+ R_0^2\tau^2\nu_{SI} + R_0^2\tau\nu_{SI}^2 - R_0\tau^2\nu_{SI}^2 + R_dR_0^2\nu_{SI} + 4R_dR_0\tau\nu_{SI} - 5R_0^3\tau - R_0^2\tau^2 - 8R_0^2\tau\nu_{SI} + 3R_0\tau^2\nu_{SI} - 4R_0\tau\nu_{SI}^2 + 2\tau^2\nu_{SI}^2 \\ &+ R_0^3 + 8R_0^2\tau + R_0^2\nu_{SI} - 2R_0\tau^2 + 12R_0\tau\nu_{SI} - 4\tau^2\nu_{SI} + 4\tau\nu_{SI}^2 - 3R_0^2 - 8R_0\tau - 2R_0\nu_{SI} + 2\tau^2 - 8\tau\nu_{SI} + 2R_0 + 4\tau). \end{aligned}$$

The coefficient $h_{q_3} = (d_2 + d_3)(d_1 + d_3)(d_1 + d_2) > 0$ is always true. Similarly, these two properties of $H_3(z)$ are available.

Property 3. *When z tends to be positive infinity, the function value of $H_3(z)$ tends to be positive infinity.*

Property 4. *$H_3(z)$ has two extreme points, denoted as $z_{31} = \frac{-h_{q_2}+\sqrt{(h_{q_2})^2-3h_{q_3}h_{q_1}}}{3h_{q_3}}$ and $z_{32} = \frac{-h_{q_2}-\sqrt{(h_{q_2})^2-3h_{q_3}h_{q_1}}}{3h_{q_3}}$. and $H_3(z)$ takes a minimum value at point z_{31} and a maximum at point z_{32}, their size relationship is:*

$$z_{3,\max} = z_{32} < z_{3,\min} = z_{31}.$$

$H_3(z_{3,\min}) = H_3(z_{31}) < 0$ ensures the emergence of Turing pattern. $z_{3,\min} = z_{31} = \frac{-h_{q_2}+\sqrt{(h_{q_2})^2-3h_{q_3}h_{q_1}}}{3h_{q_3}}$ represents a physical wave number, and thus $z_{3,\min} = z_{31} > 0$. The value of expression under the quadratic square root should be positive, scilicet, $(h_{q_2})^2 - 3h_{q_3}h_{q_1} > 0$. Thus the conditions that system (2.3) gives rise to the Turing patterns is obtained:

$$\begin{cases} (h_{q_2})^2 - 3h_{q_3}h_{q_1} > 0, \\ z_{3,\min} = z_{31} > 0, \\ H_3(z_{3,\min}) = H_3(z_{31}) < 0, \\ H_3(0) = b_1(0)b_2(0) - b_3(0) > 0, \\ b_3(0) > 0, \\ b_1(0) > 0. \end{cases} \tag{2.9}$$

3. Multiple scale analysis for turing patterns

Next, we will use the multi-scale analysis method to derive the amplitude equation [64–66]. Multi-scale analysis can determine the correspondence between each coefficient in system and the various control parameters of system. The specific process of pattern formation with control parameters in a system can be studied. It is well known that when the vibration frequency of a wave approaches the threshold k_T, the coexistence state begins to become unstable, so multi-scale analysis is used near the branch threshold of the control parameter. The core of multi-scale analysis is that according to different time scales (or spatial scales), we can separate the dynamic behavior of system, and use Fredholm's selection theorem to solve the solutions of the corresponding equations at different scales. In this paper, we choose the time delay τ as the control parameter. To this end, we first look for the critical wave number k_T, and substitute the critical wave number k_T into $b_3(k) = 0$ to obtain the branch threshold τ_T of the delay.

We firstly rewrite systems (2.2) at the equilibrium $E^* = (S^*, I^*, V^*)$ of the following form:

$$\begin{cases} \dfrac{\partial S}{\partial t} = d_1\Delta S + a_{11}S + a_{12}I + a_{13}V + N_1(S,I,V), \\ \dfrac{\partial I}{\partial t} = d_2\Delta I + a_{21}S + a_{22}I + a_{23}V + N_2(S,I,V), \\ \dfrac{\partial V}{\partial t} = d_3\Delta V + a_{31}S + a_{32}I + a_{33}V + N_3(S,I,V), \end{cases} \tag{3.1}$$

where

$$\begin{aligned} N_1(S,I,V) = &-\frac{1}{R_0(S+I)}(R_dR_0S^3\nu_{SI} + 3R_dR_0S^2I\nu_{SI} + 3R_dR_0SI^2\nu_{SI} + R_dR_0I^3\nu_{SI} - 2R_dR_0S^2\nu_{SI} - 4R_dR_0SI\nu_{SI} - 2R_dR_0I^2\nu_{SI} \\ &- R_0^2S^2 + R_0^2SV - R_0^2SI + 4R_0S^2 - R_0SV + 7R_0SI - R_0VI + 3R_0I^2 + 2S^2\nu_{SI} + 4SI\nu_{SI} + 2I^2\nu_{SI} - 3S^2 - 6SI - 3I^2), \end{aligned}$$

$$N_2(S,I,V) = -\frac{1}{R_0(S+I)}(R_0^2S^2 - R_0^2SV + R_0^2SI - 2R_0S^2 + R_0SV - 3R_0SI + R_0VI - R_0I^2 + S^2 + 2SI + I^2),$$

$$N_3(S,I,V) = 0.$$

Since near the onset $\tau = \tau_T$, the solutions of system (2.2) can be expressed as

$$U = U_u + \sum_{j=1}^{3} U_0[A_j e^{i\vec{k_j}\cdot\vec{r}} + \vec{A_j}e^{-i\vec{k_j}\cdot\vec{r}}],$$

where the term U_u is the uniform steady state, U_0 denotes the eigenvector of the linearized operator, A_j and $\vec{A_j}$ are the amplitudes with respect to the modes $\vec{k_j}$ and $-\vec{k_j}$, respectively. $\vec{k_j}$ and $-\vec{k_j}$ are a pair of oscillatory wave vectors and $|k_j| = k_T$.

According to the above formula, the solutions of (2.1) can be expanded as:

$$U^0 = \sum_{j=1}^{3} U_0[A_j e^{i\vec{k_j}\cdot\vec{r}} + \vec{A_j}e^{-i\vec{k_j}\cdot\vec{r}}].$$

Let $U = (S, I, V)^T, N = (N_1, N_2, N_3)^T$. System (3.1) can be rewritten of the following form

$$\frac{\partial U}{\partial t} = LU + N, \tag{3.2}$$

where

$$L = \begin{pmatrix} a_{11} + d_1\triangle & a_{12} & a_{13} \\ a_{21} & a_{22} + d_2\triangle & a_{23} \\ a_{31} & a_{32} & a_{33} + d_3\triangle \end{pmatrix}.$$

Let

$$L = L_T + (\tau_T - \tau)M, \tag{3.3}$$

where

$$L_T = \begin{pmatrix} a^*_{11} + d_1\triangle & a^*_{12} & a^*_{13} \\ a^*_{21} & a^*_{22} + d_2\triangle & a^*_{23} \\ a^*_{31} & a^*_{32} & a^*_{33} + d_3\triangle \end{pmatrix},$$

$$M = \begin{pmatrix} m_{11} & m_{12} & m_{13} \\ m_{21} & m_{22} & m_{23} \\ m_{31} & m_{32} & m_{33} \end{pmatrix},$$

and

$$\begin{aligned}
&a^*_{11} = a_{11}, \quad a^*_{12} = a_{12}, \quad a^*_{13} = a_{13}, \\
&a^*_{21} = a_{21}, \quad a^*_{22} = a_{22}, \quad a^*_{23} = a_{23}, \\
&a^*_{31} = a_{31}, \quad a^*_{32} = \frac{1}{\tau}, \quad a^*_{33} = -\frac{1}{\tau}, \\
&m_{11} = \frac{a_{11} - a^*_{11}}{\tau_T - \tau}, \quad m_{12} = \frac{a_{12} - a^*_{12}}{\tau_T - \tau}, \quad m_{13} = \frac{a_{13} - a^*_{13}}{\tau_T - \tau}, \\
&m_{21} = \frac{a_{21} - a^*_{21}}{\tau_T - \tau}, \quad m_{22} = \frac{a_{22} - a^*_{22}}{\tau_T - \tau}, \quad m_{23} = \frac{a_{23} - a^*_{23}}{\tau_T - \tau}, \\
&m_{31} = \frac{a_{31} - a^*_{31}}{\tau_T - \tau}, \quad m_{32} = \frac{a_{32} - a^*_{32}}{\tau_T - \tau}, \quad m_{33} = \frac{a_{33} - a^*_{33}}{\tau_T - \tau}.
\end{aligned}$$

Let

$$\tau_T - \tau = \varepsilon\tau_1 + \varepsilon^2\tau_2 + \varepsilon^3\tau_3 + o(\varepsilon^4), \tag{3.4}$$

$$U = \begin{pmatrix} S \\ I \\ V \end{pmatrix} = \varepsilon \begin{pmatrix} S_1 \\ I_1 \\ V_1 \end{pmatrix} + \varepsilon^2 \begin{pmatrix} S_2 \\ I_2 \\ V_2 \end{pmatrix} + \varepsilon^3 \begin{pmatrix} S_3 \\ I_3 \\ V_3 \end{pmatrix} + o(\varepsilon^4), \tag{3.5}$$

$$N = \varepsilon^2\widehat{h}_2 + \varepsilon^3\widehat{h}_3 + o(\varepsilon^4), \tag{3.6}$$

where

$$\widehat{h}_2 = \begin{pmatrix} \widehat{h}_{21} \\ \widehat{h}_{22} \\ 0 \end{pmatrix}, \widehat{h}_3 = \begin{pmatrix} \widehat{h}_{31} \\ \widehat{h}_{32} \\ 0 \end{pmatrix},$$

$$\begin{aligned}
\widehat{h}_{21} = &- \frac{1}{R_dR_0\nu_{SI} - R_0 - \nu_{SI} + 1}(\nu_{SI}R_d(R_dR_0S_1^2\nu_{SI} + 2R_dR_0S_1I_1\nu_{SI} + R_dR_0I_1^2\nu_{SI} - R_0^2S_1^2 + R_0^2S_1V_1 - R_0^2S_1I_1 + R_0S_1^2 - R_0S_1V_1 \\
&+ R_0S_1I_1 - R_0V_1I_1 - S_1^2\nu_{SI} - 2S_1I_1\nu_{SI} - I_1^2\nu_{SI})),
\end{aligned}$$

$$\begin{aligned}
\widehat{h}_{31} = &- \frac{1}{(R_dR_0\nu_{SI} - R_0 - \nu_{SI} + 1)^2}(\nu_{SI}R_d(2R_d^2R_0^2S_1S_2\nu_{SI}^2 + 2R_d^2R_0^2S_1I_2\nu_{SI}^2 + 2R_d^2R_0^2S_2I_1\nu_{SI}^2 + 2R_d^2R_0^2I_1I_2\nu_{SI}^2 + R_dR_0^3S_1^3\nu_{SI} \\
&- R_dR_0^3S_1^2V_1\nu_{SI} + 2R_dR_0^3S_1^2I_1\nu_{SI} - R_dR_0^3S_1V_1I_1\nu_{SI} + R_dR_0^3S_1I_1^2\nu_{SI} - 2R_dR_0^3S_1S_2\nu_{SI} + R_dR_0^3S_1V_2\nu_{SI} - R_dR_0^3S_1I_2\nu_{SI} \\
&+ R_dR_0^3S_2V_1\nu_{SI} - R_dR_0^3S_2I_1\nu_{SI} - 2R_dR_0^2S_1^3\nu_{SI} + R_dR_0^2S_1^2V_1\nu_{SI} - 5R_dR_0^2S_1^2I_1\nu_{SI} + 2R_dR_0^2S_1V_1I_1\nu_{SI} - 4R_dR_0^2S_1I_1^2\nu_{SI} \\
&+ R_dR_0^2V_1I_1^2\nu_{SI} - R_dR_0^2I_1^3\nu_{SI} - R_dR_0^2S_1V_2\nu_{SI} - R_dR_0^2S_1I_2\nu_{SI} - R_dR_0^2S_2V_1\nu_{SI} - R_dR_0^2S_2I_1\nu_{SI} - R_dR_0^2V_1I_2\nu_{SI} \\
&- R_dR_0^2V_2I_1\nu_{SI} - 2R_dR_0^2I_1I_2\nu_{SI} + R_dR_0S_1^3\nu_{SI} + 3R_dR_0S_1^2I_1\nu_{SI} - 4R_dR_0S_1S_2\nu_{SI}^2 + 3R_dR_0S_1I_1^2\nu_{SI} - 4R_dR_0S_1I_2\nu_{SI}^2
\end{aligned}$$

$$
\begin{aligned}
&- 4R_dR_0S_2I_1\nu_{SI}^2 + R_dR_0I_1^3\nu_{SI} - 4R_dR_0I_1I_2\nu_{SI}^2 + 2R_dR_0S_1S_2\nu_{SI} + 2R_dR_0S_1I_2\nu_{SI} + 2R_dR_0S_2I_1\nu_{SI} + 2R_dR_0I_1I_2\nu_{SI}\\
&+ 2R_0^3S_1S_2 - R_0^3S_1V_2 + R_0^3S_1I_2 - R_0^3S_2V_1 + R_0^3S_2I_1 + 2R_0^2S_1S_2\nu_{SI} - R_0^2S_1V_2\nu_{SI} + R_0^2S_1I_2\nu_{SI} - R_0^2S_2V_1\nu_{SI} + R_0^2S_2I_1\nu_{SI}\\
&- 4R_0^2S_1S_2 + 2R_0^2S_1V_2 - 2R_0^2S_1I_2 + 2R_0^2S_2V_1 - 2R_0^2S_2I_1 + R_0^2V_1I_2 + R_0^2V_2I_1 + R_0S_1V_2\nu_{SI} + R_0S_1I_2\nu_{SI} + R_0S_2V_1\nu_{SI}\\
&+ R_0S_2I_1\nu_{SI} + R_0V_1I_2\nu_{SI} + R_0V_2I_1\nu_{SI} + 2R_0I_1I_2\nu_{SI} + 2S_1S_2\nu_{SI}^2 + 2S_1I_2\nu_{SI}^2 + 2S_2I_1\nu_{SI}^2 + 2I_1I_2\nu_{SI}^2 + 2R_0S_1S_2 - R_0S_1V_2\\
&+ R_0S_1I_2 - R_0S_2V_1 + R_0S_2I_1 - R_0V_1I_2 - R_0V_2I_1 - 2S_1S_2\nu_{SI} - 2S_1I_2\nu_{SI} - 2S_2I_1\nu_{SI} - 2I_1I_2\nu_{SI})),
\end{aligned}
$$

$$
\widehat{h}_{22} = -\frac{1}{R_dR_0\nu_{SI} - R_0 - \nu_{SI} + 1}(\nu_{SI}R_d(R_0S_1 - R_0V_1 + R_0I_1 - S_1 - I_1)(R_0S_1 - S_1 - I_1)),
$$

$$
\begin{aligned}
\widehat{h}_{32} =& \frac{1}{(R_dR_0\nu_{SI} - R_0 - \nu_{SI} + 1)^2}(\nu_{SI}R_d(R_dR_0^3S_1^3\nu_{SI} - R_dR_0^3S_1^2V_1\nu_{SI} + 2R_dR_0^3S_1^2I_1\nu_{SI} - R_dR_0^3S_1V_1I_1\nu_{SI} + R_dR_0^3S_1I_1^2\nu_{SI}\\
&- 2R_dR_0^3S_1S_2\nu_{SI} + R_dR_0^3S_1V_2\nu_{SI} - R_dR_0^3S_1I_2\nu_{SI} + R_dR_0^3S_2V_1\nu_{SI} - R_dR_0^3S_2I_1\nu_{SI} - 2R_dR_0^2S_1^3\nu_{SI} + R_dR_0^2S_1^2V_1\nu_{SI}\\
&- 5R_dR_0^2S_1^2I_1\nu_{SI} + 2R_dR_0^2S_1V_1I_1\nu_{SI} - 4R_dR_0^2S_1I_1^2\nu_{SI} + R_dR_0^2V_1I_1^2\nu_{SI} - R_dR_0^2I_1^3\nu_{SI} + 4R_dR_0^2S_1S_2\nu_{SI} - R_dR_0^2S_1V_2\nu_{SI}\\
&+ 3R_dR_0^2S_1I_2\nu_{SI} - R_dR_0^2S_2V_1\nu_{SI} + 3R_dR_0^2S_2I_1\nu_{SI} - R_dR_0^2V_1I_2\nu_{SI} - R_dR_0^2V_2I_1\nu_{SI} + 2R_dR_0^2I_1I_2\nu_{SI} + R_dR_0S_1^3\nu_{SI}\\
&+ 3R_dR_0S_1^2I_1\nu_{SI} + 3R_dR_0S_1I_1^2\nu_{SI} + R_dR_0I_1^3\nu_{SI} - 2R_dR_0S_1S_2\nu_{SI} - 2R_dR_0S_1I_2\nu_{SI} - 2R_dR_0S_2I_1\nu_{SI} - 2R_dR_0I_1I_2\nu_{SI}\\
&+ 2R_0^3S_1S_2 - R_0^3S_1V_2 + R_0^3S_1I_2 - R_0^3S_2V_1 + R_0^3S_2I_1 + 2R_0^2S_1S_2\nu_{SI} - R_0^2S_1V_2\nu_{SI} + R_0^2S_1I_2\nu_{SI} - R_0^2S_2V_1\nu_{SI} + R_0^2S_2I_1\nu_{SI}\\
&- 6R_0^2S_1S_2 + 2R_0^2S_1V_2 - 4R_0^2S_1I_2 + 2R_0^2S_2V_1 - 4R_0^2S_2I_1 + R_0^2V_1I_2 + R_0^2V_2I_1 - 2R_0^2I_1I_2 - 4R_0S_1S_2\nu_{SI} + R_0S_1V_2\nu_{SI}\\
&- 3R_0S_1I_2\nu_{SI} + R_0S_2V_1\nu_{SI} - 3R_0S_2I_1\nu_{SI} + R_0V_1I_2\nu_{SI} + R_0V_2I_1\nu_{SI} - 2R_0I_1I_2\nu_{SI} + 6R_0S_1S_2 - R_0S_1V_2 + 5R_0S_1I_2\\
&- R_0S_2V_1 + 5R_0S_2I_1 - R_0V_1I_2 - R_0V_2I_1 + 4R_0I_1I_2 + 2S_1S_2\nu_{SI} + 2S_1I_2\nu_{SI} + 2S_2I_1\nu_{SI} + 2I_1I_2\nu_{SI} - 2S_1S_2\\
&- 2S_1I_2 - 2S_2I_1 - 2I_1I_2)).
\end{aligned}
$$

We will separate the dynamics of system according to the time scale, and let

$$
\frac{\partial}{\partial t} = \frac{\partial}{\partial T_0} + \varepsilon\frac{\partial}{\partial T_1} + \varepsilon^2\frac{\partial}{\partial T_2} + o(\varepsilon^3). \tag{3.7}
$$

Since amplitude A is a variable that varies slowly, the derivative with respect to time $\frac{\partial}{\partial T_0}$ that varies fast corresponding to the variable has no difference on the amplitude A:

$$
\frac{\partial A}{\partial t} = \varepsilon\frac{\partial A}{\partial T_1} + \varepsilon^2\frac{\partial A}{\partial T_2} + o(\varepsilon^3), \tag{3.8}
$$

where $T_0 = t, T_1 = \varepsilon t, T_2 = \varepsilon^2 t$. Which follows from system (3.2) and (3.3) that

$$
\frac{\partial U}{\partial t} = (L_T + (\tau_T - \tau)M)U + N = L_TU + (\tau_T - \tau)MU + N. \tag{3.9}
$$

Substituting Eqs. (3.4)–(3.8) into (3.9) and expanding (3.9) with different orders of ε, the following three equations can be obtained.

The order of ε:

$$
L_T\begin{pmatrix} S_1 \\ I_1 \\ V_1 \end{pmatrix} = 0. \tag{3.10}
$$

The order of ε^2:

$$
L_T\begin{pmatrix} S_2 \\ I_2 \\ V_2 \end{pmatrix} = \frac{\partial}{\partial T_1}\begin{pmatrix} S_1 \\ I_1 \\ V_1 \end{pmatrix} - \tau_1 M\begin{pmatrix} S_1 \\ I_1 \\ V_1 \end{pmatrix} - \widehat{h}_2. \tag{3.11}
$$

The order of ε^3:

$$
L_T\begin{pmatrix} S_3 \\ I_3 \\ V_3 \end{pmatrix} = \frac{\partial}{\partial T_1}\begin{pmatrix} S_2 \\ I_2 \\ V_2 \end{pmatrix} + \frac{\partial}{\partial T_2}\begin{pmatrix} S_1 \\ I_1 \\ V_1 \end{pmatrix} - \tau_1 M\begin{pmatrix} S_2 \\ I_2 \\ V_2 \end{pmatrix} - \tau_2 M\begin{pmatrix} S_1 \\ I_1 \\ V_1 \end{pmatrix} - \widehat{h}_3. \tag{3.12}
$$

Since L_T is the linear operator of system with the critical point, $(S_1, I_1, V_1)^T$ is the linear combination of eigenvectors that corresponds to the eigenvalue 0. Solving (3.10), we have

$$
\begin{pmatrix} S_1 \\ I_1 \\ V_1 \end{pmatrix} = \begin{pmatrix} l_1 \\ l_2 \\ 1 \end{pmatrix}(W_1e^{i\vec{k_1}\cdot\vec{r}} + W_2e^{i\vec{k_2}\cdot\vec{r}} + W_3e^{i\vec{k_3}\cdot\vec{r}}) + c.c., \tag{3.13}
$$

where

$$l_1 = \frac{(d_2k_T^2 - a_{22}^*)(1 + d_3\tau_T k_T^2) - a_{23}^*}{a_{21}^*}, l_2 = 1 + d_3\tau_T k_T^2,$$

and W_j is the amplitude of $e^{j\vec{k_j}\cdot\vec{r}}$ $(j = 1, 2, 3)$ with the first order perturbation, c.c. denotes the conjugate of the former terms.

For Eq. (3.11) we can obtain

$$\begin{aligned} L_T\begin{pmatrix} S_2 \\ I_2 \\ V_2 \end{pmatrix} &= \frac{\partial}{\partial T_1}\begin{pmatrix} S_1 \\ I_1 \\ V_1 \end{pmatrix} - \tau_1 M\begin{pmatrix} S_1 \\ I_1 \\ V_1 \end{pmatrix} - \widehat{h}_2 \\ &= \frac{\partial}{\partial T_1}\begin{pmatrix} S_1 \\ I_1 \\ V_1 \end{pmatrix} - \tau_1\begin{pmatrix} m_{11} & m_{12} & m_{13} \\ m_{21} & m_{22} & m_{23} \\ m_{31} & m_{32} & m_{33} \end{pmatrix}\begin{pmatrix} S_1 \\ I_1 \\ V_1 \end{pmatrix} - \begin{pmatrix} \widehat{h}_{21} \\ \widehat{h}_{22} \\ 0 \end{pmatrix} \\ &= \begin{pmatrix} F_S \\ F_I \\ F_V \end{pmatrix}. \end{aligned} \tag{3.14}$$

With the Fredholm solvability conditions, the vector function of the right-hand side of system (3.14) must be orthogonal with the zero eigenvectors of operator L_T^+ can make that Eq. (3.14) has nontrivial solution. Here L_T^+ is the adjoint operator of the operator L_T. In addition, the zero eigenvector of L_T^+ is

$$\begin{pmatrix} 1 \\ l_2^+ \\ l_3^+ \end{pmatrix} e^{-i\vec{k_j}\cdot\vec{r}}, j = 1, 2, 3,$$

where

$$l_2^+ = \frac{d_1k_T^2 - a_{11}^*}{a_{21}^*}, l_3^+ = \frac{\tau_T(d_1k_T^2 - a_{11}^*)(d_2k_T^2 - a_{22}^*) - \tau_T a_{12}^* a_{21}^*}{a_{21}^*},$$

then

$$\begin{pmatrix} 1, & l_2^+, & l_3^+ \end{pmatrix}\begin{pmatrix} F_S^j \\ F_I^j \\ F_V^j \end{pmatrix} = 0,$$

where F_S^j, F_I^j, F_V^j represent the coefficients corresponding to $e^{i\vec{k_j}\cdot\vec{r}}$ in F_S, F_I, F_V, respectively, that is to say

$$\begin{pmatrix} F_S \\ F_I \\ F_V \end{pmatrix} = \begin{pmatrix} F_S^1 \\ F_I^1 \\ F_V^1 \end{pmatrix} e^{i\vec{k_1}\cdot\vec{r}} + \begin{pmatrix} F_S^2 \\ F_I^2 \\ F_V^2 \end{pmatrix} e^{i\vec{k_2}\cdot\vec{r}} + \begin{pmatrix} F_S^3 \\ F_I^3 \\ F_V^3 \end{pmatrix} e^{i\vec{k_3}\cdot\vec{r}}.$$

Substituting (3.13) into $\widehat{h}_{21}$, $\widehat{h}_{22}$, $\widehat{h}_{31}$ and $\widehat{h}_{32}$, We only need to sort the coefficients of the $e^{-i\vec{k_j}\cdot\vec{r}}$ terms expressed as:

$$\widehat{h}_{21} \sim \widehat{h}_{21k1}\overline{W}_2\overline{W}_3 e^{i\vec{k_1}\cdot\vec{r}} + h_{21k2}\overline{W}_1\overline{W}_3 e^{i\vec{k_2}\cdot\vec{r}} + h_{21k3}\overline{W}_1\overline{W}_2 e^{i\vec{k_3}\cdot\vec{r}},$$

$$\widehat{h}_{22} \sim \widehat{h}_{22k1}\overline{W}_2\overline{W}_3 e^{i\vec{k_1}\cdot\vec{r}} + h_{22k2}\overline{W}_1\overline{W}_3 e^{i\vec{k_2}\cdot\vec{r}} + h_{22k3}\overline{W}_1\overline{W}_2 e^{i\vec{k_3}\cdot\vec{r}},$$

$$\widehat{h}_{31} \sim \widehat{h}_{31k1}\overline{W}_2\overline{W}_3 e^{i\vec{k_1}\cdot\vec{r}} + h_{31k2}\overline{W}_1\overline{W}_3 e^{i\vec{k_2}\cdot\vec{r}} + h_{31k3}\overline{W}_1\overline{W}_2 e^{i\vec{k_3}\cdot\vec{r}},$$

$$\widehat{h}_{32} \sim \widehat{h}_{32k1}\overline{W}_2\overline{W}_3 e^{i\vec{k_1}\cdot\vec{r}} + h_{32k2}\overline{W}_1\overline{W}_3 e^{i\vec{k_2}\cdot\vec{r}} + h_{32k3}\overline{W}_1\overline{W}_2 e^{i\vec{k_3}\cdot\vec{r}}.$$

By symmetry, we have that

$$h_{21k1} = h_{21k2} = h_{21k3} := \widetilde{h}_{21},$$

$$h_{22k1} = h_{22k2} = h_{22k3} := \widetilde{h}_{22},$$

$$h_{31k1} = h_{31k2} = h_{31k3} := \widetilde{h}_{31},$$

$$h_{32k1} = h_{32k2} = h_{32k3} := \widetilde{h}_{32},$$

where $\widetilde{h}_{21}, \widetilde{h}_{22}, \widetilde{h}_{31}, \widetilde{h}_{32}$ are known quantities.

Due to (3.13) and (3.14), one has

$$\begin{pmatrix} F_S^1 \\ F_I^1 \\ F_V^1 \end{pmatrix} = \begin{pmatrix} l_1 \dfrac{\partial W_1}{\partial T_1} \\ l_2 \dfrac{\partial W_1}{\partial T_1} \\ \dfrac{\partial W_1}{\partial T_1} \end{pmatrix} - \tau_1 \begin{pmatrix} m_{11}l_1 + m_{12}l_2 + m_{13} \\ m_{21}l_1 + m_{22}l_2 + m_{23} \\ m_{31}l_1 + m_{32}l_2 + m_{33} \end{pmatrix} W_1 + \begin{pmatrix} \widetilde{h}_{21} \\ \widetilde{h}_{22} \\ 0 \end{pmatrix} \overline{W}_2 \overline{W}_3, \tag{3.15}$$

$$\begin{pmatrix} F_S^2 \\ F_I^2 \\ F_V^2 \end{pmatrix} = \begin{pmatrix} l_1 \dfrac{\partial W_2}{\partial T_1} \\ l_2 \dfrac{\partial W_2}{\partial T_1} \\ \dfrac{\partial W_2}{\partial T_1} \end{pmatrix} - \tau_1 \begin{pmatrix} m_{11}l_1 + m_{12}l_2 + m_{13} \\ m_{21}l_1 + m_{22}l_2 + m_{23} \\ m_{31}l_1 + m_{32}l_2 + m_{33} \end{pmatrix} W_2 + \begin{pmatrix} \widetilde{h}_{21} \\ \widetilde{h}_{22} \\ 0 \end{pmatrix} \overline{W}_1 \overline{W}_3, \tag{3.16}$$

$$\begin{pmatrix} F_S^3 \\ F_I^3 \\ F_V^3 \end{pmatrix} = \begin{pmatrix} l_1 \dfrac{\partial W_3}{\partial T_1} \\ l_2 \dfrac{\partial W_3}{\partial T_1} \\ \dfrac{\partial W_3}{\partial T_1} \end{pmatrix} - \tau_1 \begin{pmatrix} m_{11}l_1 + m_{12}l_2 + m_{13} \\ m_{21}l_1 + m_{22}l_2 + m_{23} \\ m_{31}l_1 + m_{32}l_2 + m_{33} \end{pmatrix} W_3 + \begin{pmatrix} \widetilde{h}_{21} \\ \widetilde{h}_{22} \\ 0 \end{pmatrix} \overline{W}_1 \overline{W}_2. \tag{3.17}$$

With the Fredholm solvability condition, we get

$$\begin{cases} (l_1 + l_2 l_2^+ + l_3^+) \dfrac{\partial W_1}{\partial T_1} = \tau_1[(m_{11}l_1 + m_{12}l_2 + m_{13}) + l_2^+(m_{21}l_1 + m_{22}l_2 + m_{23}) \\ \qquad\qquad + l_3^+(m_{31}l_1 + m_{32}l_2 + m_{33})]W_1 - (\widetilde{h}_{21} + l_2^+ \widetilde{h}_{22})\overline{W}_2 \overline{W}_3, \\ (l_1 + l_2 l_2^+ + l_3^+) \dfrac{\partial W_2}{\partial T_1} = \tau_1[(m_{11}l_1 + m_{12}l_2 + m_{13}) + l_2^+(m_{21}l_1 + m_{22}l_2 + m_{23}) \\ \qquad\qquad + l_3^+(m_{31}l_1 + m_{32}l_2 + m_{33})]W_2 - (\widetilde{h}_{21} + l_2^+ \widetilde{h}_{22})\overline{W}_1 \overline{W}_3, \\ (l_1 + l_2 l_2^+ + l_3^+) \dfrac{\partial W_3}{\partial T_1} = \tau_1[(m_{11}l_1 + m_{12}l_2 + m_{13}) + l_2^+(m_{21}l_1 + m_{22}l_2 + m_{23}) \\ \qquad\qquad + l_3^+(m_{31}l_1 + m_{32}l_2 + m_{33})]W_3 - (\widetilde{h}_{21} + l_2^+ \widetilde{h}_{22})\overline{W}_1 \overline{W}_2. \end{cases} \tag{3.18}$$

System (3.18) is an amplitude equation under first-order perturbation. When the coefficient of second-order term is greater than zero, the amplitude W_i diverges. In this case, a higher-order perturbation term should be introduced to saturate it. Solve Eq. (3.11) to get

$$\begin{pmatrix} S_2 \\ I_2 \\ V_2 \end{pmatrix} = \begin{pmatrix} U_{S0} \\ U_{I0} \\ U_{V0} \end{pmatrix} + \sum_{i=1}^{3} \begin{pmatrix} U_{Si} \\ U_{Ii} \\ U_{Vi} \end{pmatrix} e^{i\vec{k}_i \cdot \vec{r}} + \sum_{i=1}^{3} \begin{pmatrix} U_{Sii} \\ U_{Iii} \\ U_{Vii} \end{pmatrix} e^{i2\vec{k}_i \cdot \vec{r}} + \begin{pmatrix} U_{S12} \\ U_{I_1 2} \\ U_{V12} \end{pmatrix} e^{i(k_1 \vec{-} k_2)\cdot \vec{r}} + \begin{pmatrix} U_{S23} \\ U_{I23} \\ U_{V23} \end{pmatrix} e^{i(k_2 \vec{-} k_3)\cdot \vec{r}} + \begin{pmatrix} U_{S31} \\ U_{I31} \\ U_{V31} \end{pmatrix} e^{i(k_3 \vec{-} k_1)\cdot \vec{r}} + c.c., \tag{3.19}$$

where

$$U_{S0} = u_{S0}(|W_1|^2 + |W_2|^2 + |W_3|^2),$$

$$U_{I0} = u_{I0}(|W_1|^2 + |W_2|^2 + |W_3|^2),$$

$$U_{V0} = u_{V0}(|W_1|^2 + |W_2|^2 + |W_3|^2),$$

$$U_{Si} = l_1 U_{Vi}, U_{Ii} = l_2 U_{Vi},$$

$$U_{Sii} = u_{Sii} W_i^2, U_{Iii} = u_{Iii} W_i^2, U_{Vii} = u_{Vii} W_i^2,$$

$$U_{S12} = u_{S12} W_1 \overline{W}_2, U_{I_1 2} = u_{I_1 2} W_1 \overline{W}_2, U_{V12} = u_{V12} W_1 \overline{W}_2,$$

$$U_{S23} = u_{S12}W_2\overline{W}_3, U_{I23} = u_{I_12}W_2\overline{W}_3, U_{V23} = u_{V12}W_2\overline{W}_3,$$

$$U_{S31} = u_{S12}W_3\overline{W}_1, U_{I31} = u_{I_12}W_3\overline{W}_1, U_{V31} = u_{V12}W_3\overline{W}_1,$$

where u_{S0}, u_{I0}, u_{V0}, u_{Sii}, u_{Iii}, u_{Vii}, u_{S12}, u_{I12}, u_{V12} are known.

Substituting the solutions (3.13) and (3.19) of the upper two-level perturbation equation into (3.12), and using the Fredholm solvability condition, we get

$$\begin{cases}
(l_1 + l_2l_2^+ + l_3^+)\left(\dfrac{\partial U_{V1}}{\partial T_1} + \dfrac{\partial W_1}{\partial T_2}\right) = \tau_1[(m_{11}l_1 + m_{12}l_2 + m_{13}) + l_2^+(m_{21}l_1 + m_{22}l_2 + m_{23}) \\
\qquad + l_3^+(m_{31}l_1 + m_{32}l_2 + m_{33})]U_{V1} \\
\qquad + \tau_2[(m_{11}l_1 + m_{12}l_2 + m_{13}) + l_2^+(m_{21}l_1 + m_{22}l_2 + m_{23}) \\
\qquad + l_3^+(m_{31}l_1 + m_{32}l_2 + m_{33})]W_1 - (G_1 + l_2^+G_2)W_1 \\
\qquad + \widetilde{h}_{31-32}(\overline{U}_{V3}\overline{W}_2 + \overline{U}_{V2}\overline{W}_3), \\
(l_1 + l_2l_2^+ + l_3^+)\left(\dfrac{\partial U_{V2}}{\partial T_1} + \dfrac{\partial W_2}{\partial T_2}\right) = \tau_1[(m_{11}l_1 + m_{12}l_2 + m_{13}) + l_2^+(m_{21}l_1 + m_{22}l_2 + m_{23}) \\
\qquad + l_3^+(m_{31}l_1 + m_{32}l_2 + m_{33})]U_{V2} \\
\qquad + \tau_2[(m_{11}l_1 + m_{12}l_2 + m_{13}) + l_2^+(m_{21}l_1 + m_{22}l_2 + m_{23}) \\
\qquad + l_3^+(m_{31}l_1 + m_{32}l_2 + m_{33})]W_2 - (G_1 + l_2^+G_2)W_2 \\
\qquad + \widetilde{h}_{31-32}(\overline{U}_{V3}\overline{W}_1 + \overline{U}_{V1}\overline{W}_3), \\
(l_1 + l_2l_2^+ + l_3^+)\left(\dfrac{\partial U_{V3}}{\partial T_1} + \dfrac{\partial W_3}{\partial T_2}\right) = \tau_1[(m_{11}l_1 + m_{12}l_2 + m_{13}) + l_2^+(m_{21}l_1 + m_{22}l_2 + m_{23}) \\
\qquad + l_3^+(m_{31}l_1 + m_{32}l_2 + m_{33})]U_{V3} \\
\qquad + \tau_2[(m_{11}l_1 + m_{12}l_2 + m_{13}) + l_2^+(m_{21}l_1 + m_{22}l_2 + m_{23}) \\
\qquad + l_3^+(m_{31}l_1 + m_{32}l_2 + m_{33})]W_3 - (G_1 + l_2^+G_2)W_3 \\
\qquad + \widetilde{h}_{31-32}(\overline{U}_{V1}\overline{W}_2 + \overline{U}_{V2}\overline{W}_1),
\end{cases} \tag{3.20}$$

where

$$G_1 = g_{11}|W_1|^2 + g_{123}(|W_2|^2 + |W_3|^2),$$

$$G_2 = g_{21}|W_1|^2 + g_{223}(|W_2|^2 + |W_3|^2),$$

$g_{11}, g_{123}, g_{21}, g_{223}, \widetilde{h}_{31-32}$ are known.

Let $A_i = A_i^S = \frac{l_1}{l_2}A_i^I = l_1A_i^V$ be the coefficient of $e^{i\vec{k_j}\cdot\vec{r}}$ $(j = 1, 2, 3)$, then

$$\begin{pmatrix} A_i^S \\ A_i^I \\ A_i^V \end{pmatrix} = \varepsilon \begin{pmatrix} l_1 \\ l_2 \\ 1 \end{pmatrix} W_i + \varepsilon^2 \begin{pmatrix} l_1 \\ l_2 \\ 1 \end{pmatrix} U_{Vi} + o(\varepsilon^3), i = 1, 2, 3. \tag{3.21}$$

Multiplying (3.18) and (3.20) by ε and ε^2, using (3.8) and (3.21) to combine variables, and obtaining the following amplitude equation

$$\begin{cases}
\varrho\dfrac{\partial A_1}{\partial t} = \widetilde{\mu}A_1 + \widetilde{h}\overline{A}_2\overline{A}_3 - [g_1|A_1|^2 + g_2(|A_2|^2 + |A_3|^2)]A_1, \\
\varrho\dfrac{\partial A_2}{\partial t} = \widetilde{\mu}A_2 + \widetilde{h}\overline{A}_1\overline{A}_3 - [g_1|A_2|^2 + g_2(|A_1|^2 + |A_3|^2)]A_2, \\
\varrho\dfrac{\partial A_3}{\partial t} = \widetilde{\mu}A_3 + \widetilde{h}\overline{A}_1\overline{A}_2 - [g_1|A_3|^2 + g_2(|A_1|^2 + |A_2|^2)]A_3,
\end{cases} \tag{3.22}$$

where

$$\varrho = \frac{\eta}{2\zeta\tau_T}, \widetilde{\mu} = \frac{\tau_T - \tau}{\tau_T}, \widetilde{h} = \frac{\widetilde{h}_{31--32}}{l_1\zeta\tau_T},$$

$$g_1 = \frac{g_{11} + l_2^+g_{21}}{2l_1^2\zeta\tau_T}, g_2 = \frac{g_{123} + l_2^+g_{223}}{2l_1^2\zeta\tau_T},$$

$$\eta = l_1 + l_2l_2^+ + l_3^+,$$

$$\zeta = (m_{11}l_1 + m_{12}l_2 + m_{13}) + l_2^+(m_{21}l_1 + m_{22}l_2 + m_{23}) + l_3^+(m_{31}l_1 + m_{32}l_2 + m_{33}).$$

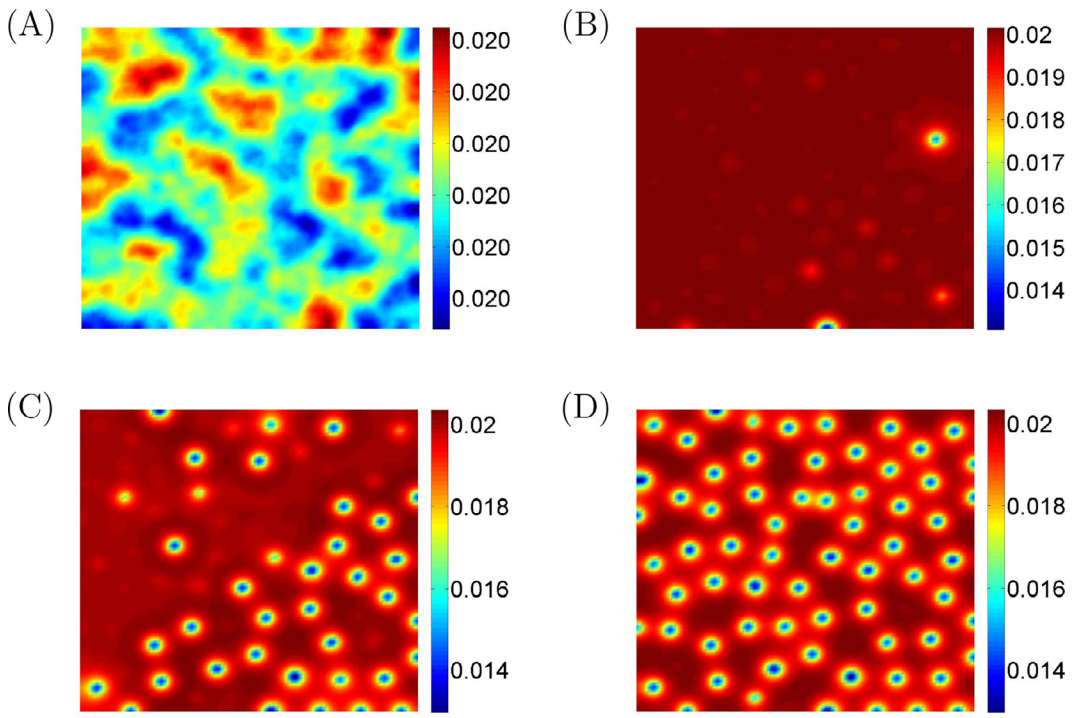

Fig. 1. The evolution of the spatial density of infected over time when the parameter $\tau = 1.67$. The direction of time evolution is $(A) \rightarrow (B) \rightarrow (C) \rightarrow (D)$.

4. Numerical results

Since the analytical solution of the reaction-diffusion equation with nonlocal delay cannot be obtained, we use the numerical format to solve the problem. Here we use the finite-difference format to numerically simulate the solution. The two-dimensional space area is selected as [0, 100] $\times$ [0, 100], the space step is taken as $\Delta h = 1$, the time interval is taken as [0,5000], and the time step is $\Delta t = 0.05$. For the non-local delay reaction-diffusion equation, we focus on the influence of non-local delay for infectious diseases. In the simulation, we choose the delay τ as the control parameter, and use the amplitude equation obtained by multi-scale theory to obtain a rich Turing pattern. For the amplitude equation (3.22), different parameters correspond to different pattern structures. The following six sets of graphs reveal the dynamics of a SI infectious disease model with non-local delay.

Figs. 1 and 2 show the time evolution of the infected populations as $\tau = 1.67$ and $\tau = 6.36$, respectively. The time evolution direction is $A - B - C - D$. D is the steady-state graph, and the other parameters have the same value. The parameter is taken as $R_d = 2,\ R_0 = 1.1,\ d_1 = 0.01,\ d_2 = 2.3,\ d_3 = 1,\ \nu_{SI} = 0.14$. As seen from these two figures, spotted pattern will domain the spatial space as time is long enough.

Fig. 3 depicts the values when the infected population is in an equilibrium state with different non-local delays. It can be clearly seen that the isolation degree of the spatial pattern increases with the increase of its value, which leads to the blocking of the diffusion pathway and is not conducive to the spread of infectious diseases. That is to say that, non-local delays inhibits the propagation of the diseases. In order to better see the spatial distribution of infected populations, we present the distribution of the infective in Fig. 4 in three-dimensional spatial space.

Fig. 5 shows the time series of the density of the infected population corresponding to different positions (five positions were chosen at random) in space. It can be seen that when time is sufficient and large, the density of infected population tends to approach a stable state. Fig. 6 shows the effects of different non-local delays on the average density of infected populations. As a whole (or as a general trend), the average density of patients decreases as time delay increases. This means that time delay is not conducive to the spread of infectious diseases, which is consistent with the conclusion in Figs. 3 and 4.

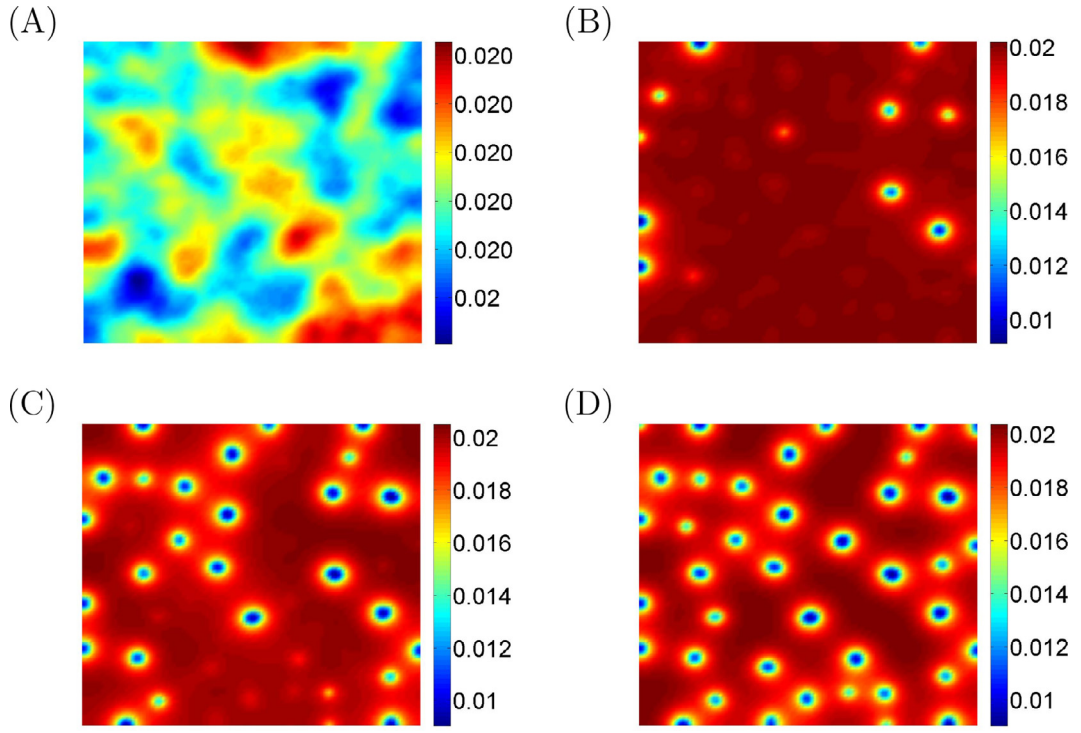

Fig. 2. The evolution of the spatial density of infected over time when the parameter $\tau = 6.36$. The direction of time evolution is $(A) \rightarrow (B) \rightarrow (C) \rightarrow (D)$.

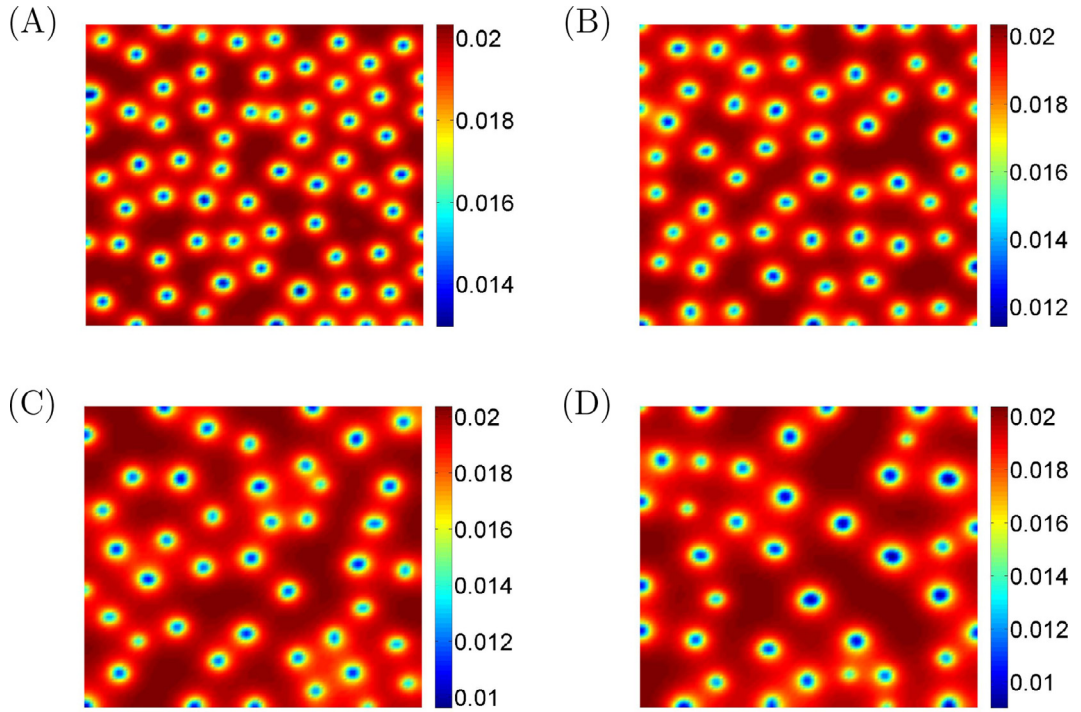

Fig. 3. If other parameters are the same, different time delays correspond to Turing Patterns (In two dimensions). (A) $\tau = 1.67$; (B) $\tau = 3.01$; (C) $\tau = 5.02$; (D) $\tau = 6.36$.

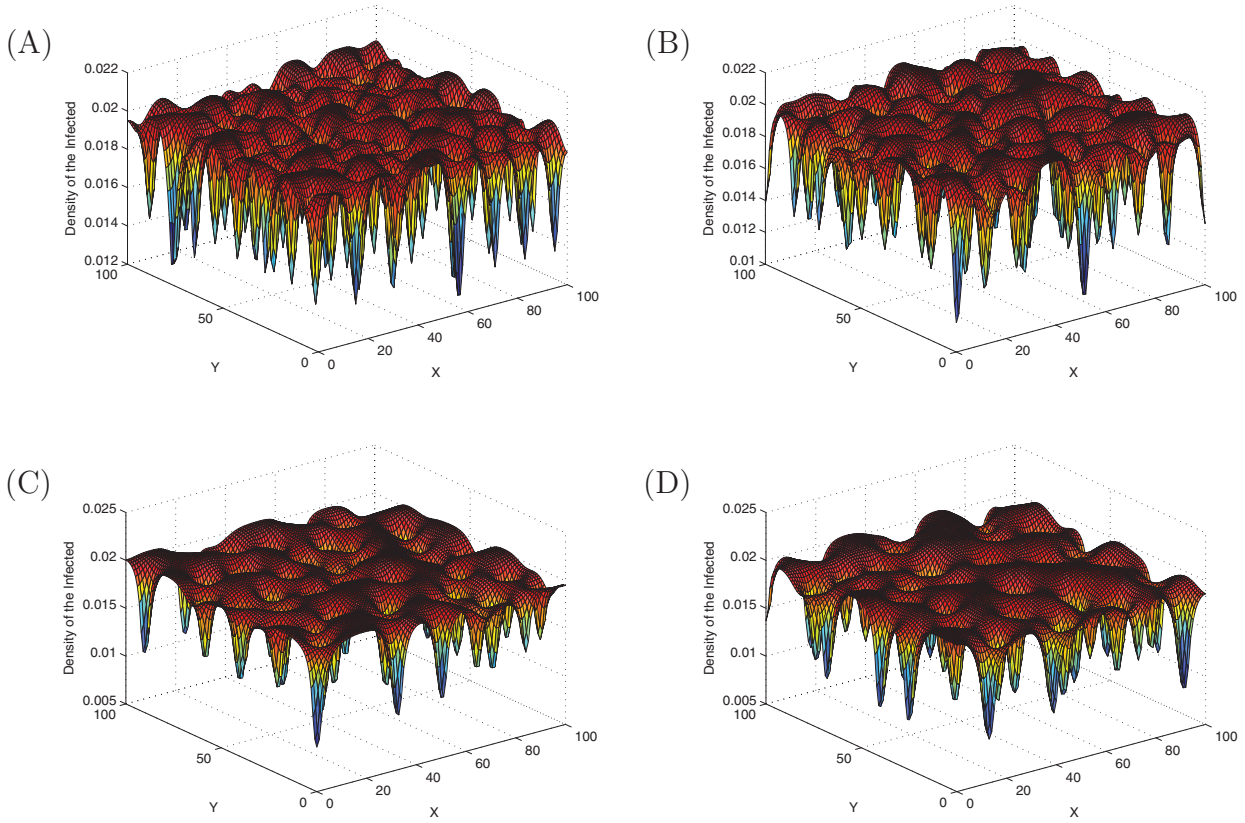

Fig. 4. If other parameters are the same, different time delays correspond to Turing Patterns (In three dimensions). (A) $\tau = 1.67$; (B) $\tau = 3.01$; (C) $\tau = 5.02$; (D) $\tau = 6.36$.

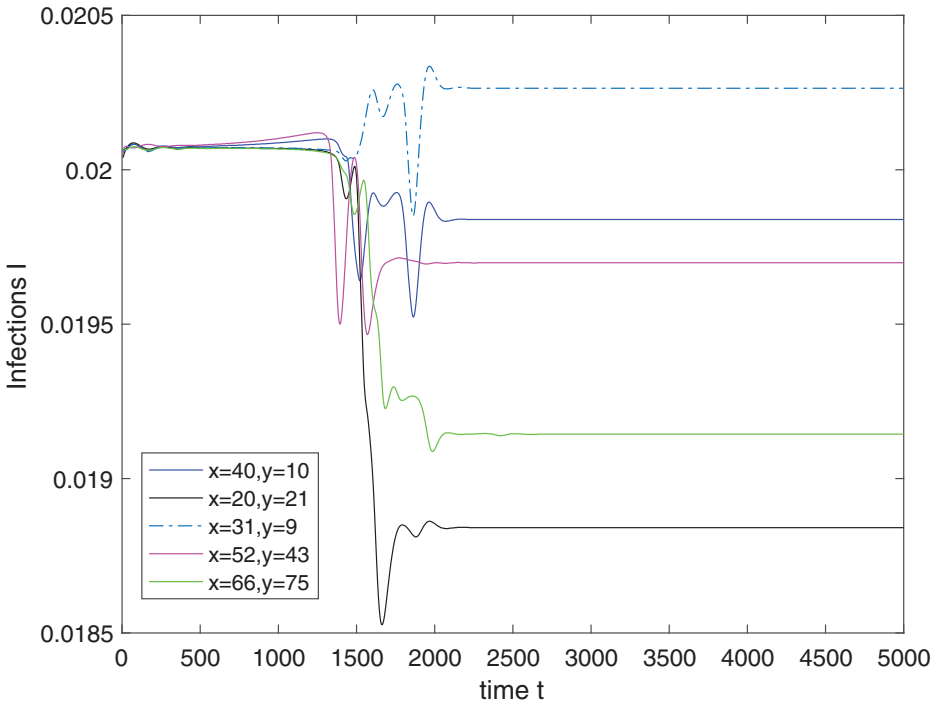

Fig. 5. The density-time evolution map of the infected populations at different spatial locations. Parameter values: $R_d = 2$, $R_0 = 1.1$, $d_1 = 0.01$, $d_2 = 2.3$, $d_3 = 1$, $\nu_{SI} = 0.14$ and $\tau = 4$.

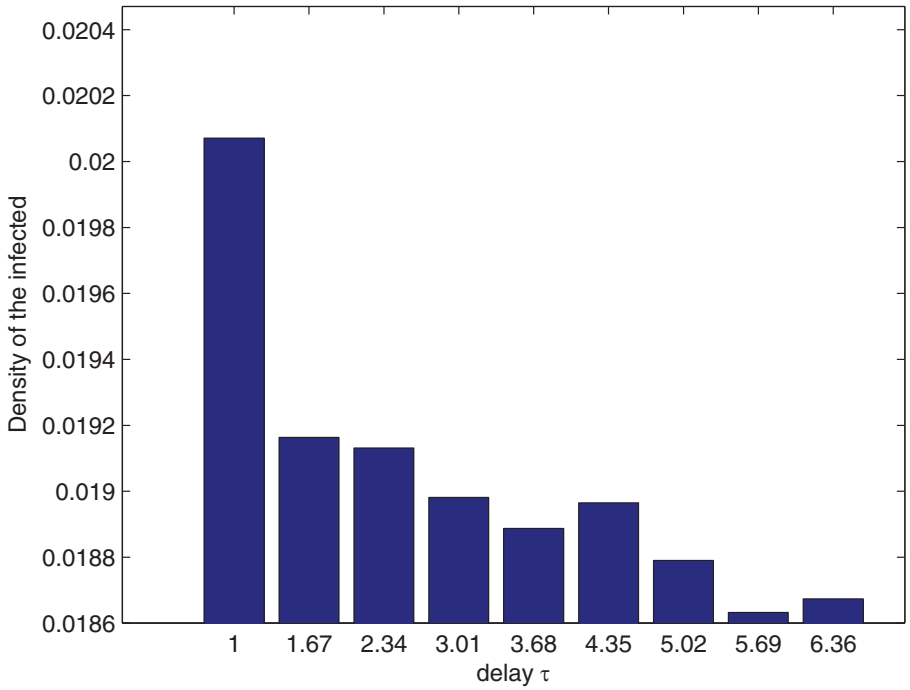

Fig. 6. The steady state value of infected populations with respect to non-local delay parameter. Other parameter values: $R_d = 2$, $R_0 = 1.1$, $d_1 = 0.01$, $d_2 = 2.3$, $d_3 = 1$, and $\nu_{SI} = 0.14$.

5. Conclusions

In this paper, we research an two-dimensional epidemic model with nonlocal delay reaction-diffusion equation. This model can be transformed into a three-dimensional reaction-diffusion equation by taking weak kernel. Firstly, the model is linearly analyzed, and then the amplitude equation is derived using multi-scale analysis theory. A steady-state solution of the amplitude equation corresponds to a pattern structure. In this paper, an infectious pattern with point structure is found. When the delay was selected as the control parameter, it was found that the increase of the delay, the isolation degree of the infectious disease pattern became smaller, and the disease was not easy to spread. It can be seen from Figs. 3 and 4 that the number of points in the dot pattern increases and becomes less and less. From Fig. 6, one can obtain that the increase in the average density of the spatially ill patients is generally reduced. The nonlocal delay term plays a very important role in the transmission of infectious diseases. It can be seen from Fig. 6 that the average density of infected people in space generally decreases with the increase of time delay, and the nonlocal delay term plays a very important role in the process of infectious disease transmission. The nonlocal movement of the population can be reduced to control the occurrence of diseases, which provides a certain theoretical basis for disease prevention and control.

Although this work posed an epidemic model with both time and space in a general form, the results can be applied to many realistic models, such as influenza [70–73], which has a typical feature of nonlocal interactions that can be transmitted by aircraft over long distances or by direct contact over short distances. Additionally, pattern structures of disease can identify the hot area of disease spread and reveal the trends of disease transmission. If data analysis is combined with the mathematical models, then one can provide accurate measures for prevention and control of infectious diseases. It should be noted that our results can be extended to other related research fields, such as ecosystems including predator-prey interactions [74–76], vegetation patterns and so on [77–80].

Acknowledgments

The project is funded by the Key Area R & D Program of Guangdong Province No. 2019B010137004, National Natural Science Foundation of China under Grant Nos. 11671241, U1803263, 11931015, Key Area R & D Program of Shaanxi Province (No. 2019ZDLGY17-07) the Fundamental Research Funds for the Central Universities 3102019PJ006, Program for the Outstanding Innovative Teams (OIT) of Higher Learning Institutions of Shanxi, Natural Science Foundation of Shanxi Province Grant nos. 201901D111322 and 201801D221003, China Postdoctoral Science Foundation under Grant no. 2017M621110, Outstanding Young Talents Support Plan of Shanxi province, Selective Support for Scientific and Technological Activities of Overseas Scholars of Shanxi province, and Program for the (Reserved) Discipline Leaders of Taiyuan Institute of Technology.

References

[1] D. Liu, W.F. Shi, Y. Shi, D.Y. Wang, Origin and diversity of novel avian influenza a h7n9 viruses causing human infection: phylogenetic, structural, and coalescent analyses, Lancet 381 (2013) 1926–1932.
[2] M. Keeling, B. Grenfell, Disease extinction and community size: modeling the persistence of measles, Science 275 (1997) 65–67.
[3] M.J. Keeling, P. Rohani, Modeling Infectious Diseases in Humans and Animals, Princeton University Press, Princeton, 2007.
[4] G.-Q. Sun, J.-H. Xie, S.-H. Huang, Z. Jin, M.-T. Li, L. Liu, Transmission dynamics of cholera: mathematical modeling and control strategies, Commun. Nonlinear Sci. Numer. Simulat. 45 (2017) 235–244.
[5] L. Li, J. Zhang, C. Liu, H.T. Zhang, Y. Wang, Z. Wang, Analysis of transmission dynamics for Zika virus on networks, Appl. Math. Comput. 347 (2019) 566–577.
[6] Y. Xing, L.-P. Song, G.-Q. Sun, Z. Jin, J. Zhang, Assessing reappearance factors of h7n9 avian influenza in china, Appl. Math. Comput. 309 (2017) 192–204.
[7] M.Y. Li, H.L. Smith, L. Wang, Global dynamics of an SEIR epidemic model with vertical transmission, SIAM J. Appl. Math. 62 (2001) 58–69.
[8] M. Fan, M.Y. Li, K. Wang, Global stability of an SEIS epidemic model with recruitment and a varying total population size, Math. Biosci. 170 (2001) 199–208.
[9] H.M. Wei, X.Z. Li, M. Martcheva, An epidemic model of a vector-borne disease with direct transmission and time delay, J. Math. Anal. Appl. 342 (2008) 895–908.
[10] Z. Ma, J. Liu, J. Li, Stability analysis for differential infectivity epidemic models, Nonlinear Anal.: Real World Appl. 4 (2003) 841–856.
[11] J. Mena-Lorca, H.W. Hethcote, Dynamic models of infectious diseases as regulators of population sizes, J. Math. Biol. 30 (1992) 693–716.
[12] H.R. Thieme, Uniform persistence and permanence for nonautonomous semiflows in population biology, Math. Biosci. 166 (2000) 173–201.
[13] H.R. Thieme, Uniform weak implies uniform strong persistence for non-autonomous semiflows, Proc. Amer. Math. Soc. 127 (1999) 2395–2403.
[14] J. Cui, X. Mu, H. Wan, Saturation recovery leads to multiple endemic equilibria and backward bifurcation, J. Theor. Biol. 254 (2008) 275–283.
[15] S. Gao, L. Chen, J.J. Nieto, A. Torres, Analysis of a delayed epidemic model with pulse vaccination and saturation incidence, Vaccine 24 (2006) 6037–6045.
[16] X. Song, Y. Jiang, H. Wei, Analysis of a saturation incidence SVEIRS epidemic model with pulse and two time delays, Appl. Math. Comput. 214 (2009) 381–390.
[17] R. Xu, Z. Ma, Global stability of a delayed SEIRS epidemic model with saturation incidence rate, Nonlinear Dyn. 61 (2010) 229–239.
[18] S. Gao, Y. Liu, J.J. Nieto, H. Andrade, Seasonality and mixed vaccination strategy in an epidemic model with vertical transmission, Math. Comput. Simul. 81 (2011) 1855–1868.
[19] T. Zhang, Z. Teng, Pulse vaccination delayed SEIRS epidemic model with saturation incidence, Appl. Math. Model. 32 (2008) 1403–1416.
[20] R. Xu, Z. Ma, Z. Wang, Global stability of a delayed SIRS epidemic model with saturation incidence and temporary immunity, Comput. Math. Appl. 59 (2010) 3211–3221.
[21] W.M. Liu, S.A. Levin, Y. Iwasa, Influence of nonlinear incidence rates upon the behavior of SIRS epidemiological models, J. Math. Biol. 23 (1986) 187–204.
[22] M.E. Alexander, S.M. Moghadas, Periodicity in an epidemic model with a generalized non-linear incidence, Math. Biosci. 189 (2004) 75–96.
[23] W.R. Derrick, P. van den Driessche, A disease transmission model in a nonconstant population, J. Math. Biol. 31 (1993) 495–512.
[24] H.W. Hethcote, The mathematics of infectious disease, SIAM Rev. 42 (2000) 599–653.
[25] H.W. Hethcote, S.A. Levin, Periodicity in Epidemiological Models, in: L. Gross, T.G. Hallam, S.A. Levin (Eds.), Applied Mathematical Ecology, Springer-Verlag, Berlin, 1989, p. 193.
[26] H.W. Hethcote, P. van den Driessche, Some epidemiological models with nonlinear incidence, J. Math. Biol. 29 (1991) 271–287.
[27] S. Ruan, W. Wang, Dynamical behavior of an epidemic model with a nonlinear incidence rate, J. Diff. Eqs. 188 (2003) 135–163.
[28] R. Bhattacharyya, B. Mukhopadhyay, On an epidemiological model with nonlinear infection incidence: local and global perspective, Appl. Math. Model. 35 (2011) 3166–3174.
[29] X. Zhang, X. Liu, Backward bifurcation and global dynamics of an SIS epidemic model with general incidence rate and treatment, Nonlinear Anal. Real World Appl. 10 (2009) 565–575.
[30] L.M. Cai, X.Z. Li, Analysis of a SEIV epidemic model with a nonlinear incidence rate, Appl. Math. Model. 33 (2009) 2919–2926.
[31] E. Barbera, G. Consolo, G. Valenti, Spread of infectious diseases in a hyperbolic reaction-diffusion susceptible-infected-removed model, Phys. Rev. E 88 (2013) 052719.
[32] A. Lahrouz, L. Omari, D. Kiouach, A. Belmaati, Complete global stability for an SIRS epidemic model with generalized non-linear incidence and vaccination, Appl. Math. Comput. 218 (2012) 6519–6525.
[33] M.E. Alexander, S.M. Moghadas, Bifurcation analysis of an SIRS epidemic model with generalized incidence, SIAM J. Appl. Math. 65 (2005) 1794–1816.
[34] Y.N. Xiao, S.Y. Tang, Dynamics of infection with nonlinear incidence in a simple vaccination model, Nonlinear Anal. Real World Appl. 11 (2010) 4154–4163.
[35] G.-Q. Sun, Z. Jin, Q.X. Liu, L. Li, Pattern formation in a spatial S-I model with non-linear incidence rates, J. Stat. Mech. 11 (2007) P11011.
[36] G.-Q. Sun, M. Jusup, Z. Jin, Y. Wang, Z. Wang, Pattern transitions in spatial epidemics: mechanisms and emergent properties, Phys. Life Rev. 19 (2016) 43–73.
[37] Q.-X. Liu, Z. Jin, M.X. Liu, Spatial organization and evolution period of the epidemic model using cellular automata, Phys. Rev. E 74 (2006) 031110.
[38] G.Q. Sun, Pattern formation of an epidemic model with diffusion, Nonlinear Dyn. 69 (2012) 1097–1104.
[39] W. Wang, H. Liu, Z. Li, Z. Guo, Y. Yang, Invasion dynamics of epidemic with the Allee effect, BioSystems 105 (2011) 25–33.
[40] L. Li, Patch invasion in a spatial epidemic model, Appl. Math. Comput. 258 (2015) 342–349.
[41] S. Berres, R. Ruiz-Baier, A fully adaptive numerical approximation for a two-dimensional epidemic model with nonlinear cross-diffusion, Nonlinear Anal. 12 (2011) 2888–2903.
[42] R. Ruiz-Baier, C. Tian, Mathematical analysis and numerical simulation of pattern formation under cross-diffusion, Nonlinear Anal. 14 (2013) 601–612.
[43] Z.C. Wang, W.T. Li, S. Ruan, Traveling fronts in monostable equations with nonlocal delayed effects, J. Dyn. Differ. Equ. 20 (2008) 573–607.
[44] Z. Ma, R. Yuan, Traveling wave solutions of a nonlocal dispersal SIRS model with spatio-temporal delay, Int. J. Biomath. 10 (2017) 1750071.
[45] H. Cheng, R. Yuan, Traveling waves of a nonlocal dispersal Kermack–Mckendrick epidemic model with delayed transmission, J. Evol. Equ. 17 (2017) 979–1002.
[46] Y. Lou, X.Q. Zhao, A reaction-diffusion Malaria model with incubation period in the vector population, J. Math. Biol. 62 (2011) 543–568.
[47] L. Zhang, W.T. Li, S.L. Wu, Multi-type entire solutions in a nonlocal dispersal epidemic model, J. Dyn. Differ. Equ. 28 (2016) 189–224.
[48] Z.C. Wang, J. Wu, Travelling waves of a diffusive Kermack–Mckendrick epidemic model with non-local delayed transmission, Proc. Roy. Soc. A 466 (2009) 237–261.
[49] Y. Li, W.T. Li, F.Y. Yang, Traveling waves for a nonlocal dispersal SIR model with delay and external supplies, Appl. Math. Comput. 247 (2014) 723–740.
[50] J.B. Wang, W.T. Li, F.Y. Yang, Traveling waves in a nonlocal dispersal SIR model with nonlocal delayed transmission, Commun. Nonlinear Sci. 27 (2015) 136–152.
[51] S.L. Wu, S.Y. Liu, Asymptotic speed of spread and traveling fronts for a nonlocal reaction-diffusion model with distributed delay, Appl. Math. Model. 33 (2009) 2757–2765.
[52] S.A. Gourley, R. Liu, J. Wu, Some vector borne diseases with structured host populations: extinction and spatial spread, SIAM J. Appl. Math. 67 (2007) 408–433.
[53] S.L. Wu, P. Weng, Entire solutions for a multi-type SIS nonlocal epidemic model in R or Z, J. Math. Anal. Appl. 394 (2012) 603–615.

[54] S.L. Wu, G. Chen, Uniqueness and exponential stability of traveling wave fronts for a multi-type SIS nonlocal epidemic model, Nonlinear Anal. Real World Appl. 36 (2017) 267–277.
[55] F.Y. Yang, W.T. Li, Traveling waves in a nonlocal dispersal SIR model with critical wave speed, J. Math. Anal. Appl. 458 (2018) 1131–1146.
[56] Q. Tang, J. Ge, Z. Lin, An SEI-SI avian-human influenza model with diffusion and nonlocal delay, Appl. Math. Comput. 247 (2014) 753–761.
[57] B.C. Tian, R. Yuan, Traveling waves for a diffusive SEIR epidemic model with non-local reaction, Appl. Math. Model. 50 (2017) 432–449.
[58] C.C. Zhu, W.T. Li, F.Y. Yang, Traveling waves in a nonlocal dispersal SIRH model with relapse, Comput. Math. Appl. 73 (2017) 1707–1723.
[59] Z. Zhen, J. Wei, J. Zhou, L. Tian, Wave propagation in a nonlocal diffusion epidemic model with nonlocal delayed effects, Appl. Math. Comput. 339 (2018) 15–37.
[60] C. Wu, D. Xiao, Travelling wave solutions in a non-local and time-delayed reactioncdiffusion model, IMA J. Appl. Math. 78 (2013) 1290–1317.
[61] X. Yu, C. Wu, P. Weng, Traveling waves for a SIRS model with nonlocal diffusion, Int. J. Biomath. 5 (2012) 1250036.
[62] Y. Peng, T. Zhang, M.O. Tade, Existence of travelling fronts in a diffusive vector disease model with spatio-temporal delay, Nonlinear Anal. 11 (2010) 2472–2478.
[63] Z.-G. Guo, L.-P. Song, G.-Q. Sun, C. Li, Z. Jin, Pattern dynamics of an SIS epidemic model with nonlocal delay, Int. J. Bifurcat. Chaos 29 (2019) 1950027.
[64] M.C. Cross, P.C. Hohenberg, Pattern formation outside of equilibrium, Rev. Mod. Phys. 65 (1993) 851–1112.
[65] V. Dufiet, J. Boissonade, Conventional and unconventional turing patterns, J. Chem. Phys. 96 (1992) 664–673.
[66] B.S. Han, Z.C. Wang, Turing patterns of a Lotka–Volterra competitive system with nonlocal delay, Int. J. Bifurcat. Chaos 28 (2018) 1830021.
[67] F.M. Hilker, M. Langlais, H. Malchow, The Allee effect and infectous diseases: extinction, multistability and the (dis-)appearance of oscillations, Am. Nat. 173 (2009) 72–88.
[68] L.L. Cai, G.T. Chen, D.M. Xiao, Multiparametric bifurcations of an epidemiological model with strong Allee effect, J. Math. Biol. 67 (2013) 185–215.
[69] L.Q. Gao, H.W. Hethcote, Disease transmission models with density-dependent demographics, J. Math. Biol. 30 (1992) 717–731.
[70] G.J. Smith, D. Vijaykrishna, J. Bahl, S.J. Lycett, M. Worobey, O.G. Pybus, J.M. Peiris, Origins and evolutionary genomics of the 2009 swine-origin h1n1 influenza a epidemic, Nature 459 (2009) 1122–1128.
[71] C. Fraser, C.A. Donnelly, S. Cauchemez, W.P. Hanage, M.D.V. Kerkhove, T.D. Hollingsworth, T. Jombart, Pandemic potential of a strain of influenza a (h1n1): early findings, Science 324 (2009) 1557–1561.
[72] B. Olsen, V.J. Munster, A. Wallensten, J. Waldenstrm, A.D. Osterhaus, R.A. Fouchier, Global patterns of influenza a virus in wild birds, Science 312 (2006) 384–388.
[73] K.S. Li, Y. Guan, J. Wang, G.J.D. Smith, K.M. Xu, L. Duan, A.T.S. Estoepangestie, Genesis of a highly pathogenic and potentially pandemic h5n1 influenza virus in eastern asia, Nature 430 (2004) 209–213.
[74] L. Li, Z. Jin, J. Li, Periodic solutions in a herbivore-plant system with time delay and spatial diffusion, Appl. Math. Model. 40 (2016) 4765–4777.
[75] G.-Q. Sun, S.-L. Wang, Q. Ren, Z. Jin, Y.P. Wu, Effects of time delay and space on herbivore dynamics: linking inducible defenses of plants to herbivore outbreak, Sci. Rep. 5 (2015) 11246.
[76] A.B. Medvinsky, S.V. Petrovskii, I.A. Tikhonova, H. Malchow, B.L. Li, Spatio-temporal complexity of plankton and fish dynamics in simple model ecosystems, SIAM Rev. 44 (2002) 311–370.
[77] G.-Q. Sun, C.-H. Wang, Z.Y. Wu, Pattern dynamics of a Gierer–Meinhardt model with spatial effects, Nonlinear Dyn. 88 (2017) 1385–1396.
[78] M. Rietkerk, S. Dekker, P. de Ruiter, J. van de Koppel, Self-organized patchiness and catastrophic shifts in ecosystems, Science 305 (2004) 1926–1929.
[79] G.-Q. Sun, C.-H. Wang, L.-L. Chang, Y.-P. Wu, L. Li, Z. Jin, Effects of feedback regulation on vegetation patterns in semi-arid environments, Appl. Math. Model. 61 (2018) 200–215.
[80] S. Getzin, H. Yizhaq, B. Bell, T.E. Erickson, et al., Discovery of fairy circles in Australia supports self-organization theory, Proc. Natl. Acad. Sci. 113 (2016) 3551–3556.